

Experimental and computational study of performance characteristics in S-shaped diffuser

Arun Gupta¹, Hardial Singh^{2*}

¹ Capgemini Engineering, Greater Noida, India

² Department of Mechanical Engineering, Amity University Haryana, India

*e-mail address: hardialsingh3@gmail.com

Abstract— Experimental and computational studies were carried out on the S-shaped diffusers to determine the impact of the change in curvature of a straight-wall diffuser. A straight diffuser became a curved diffuser at completely different angles as their similar upper and lower limbs (30°/30°, 45°/45°). The diffuser profile equations were computed using the MATLAB/Simulink v2017 programme. The S-shaped diffuser has a distinct feature with a square inlet and a rectangular outlet. The centerline length is constant for all the diffusers. The S-shaped diffusers were compared to straight-wall diffuser with the same inlet velocity and Reynolds number in terms of static pressure recovery and total pressure loss coefficients. The findings show that as the curve of the diffuser increases, the flow uniformity at the exit decreases, the static pressure loss rises at the inflection plane, and the total pressure loss coefficient increases.

Keywords- *S-shaped diffuser, Static pressure recovery coefficient, Total pressure loss coefficient, Static pressure, MATLAB Simulink.*

I. INTRODUCTION

A diffuser is a device that reduces the velocity of a moving fluid while increasing the static pressure at the expense of the fluid's kinetic energy. There are many distinct types of diffusers, such as radial, axial, and curved diffusers, depending on the geometrical design, and they have a wide range of applications in various industries. Review of flow parameters within these diffusers is of primary motivation to researchers within the fluid mechanics area.

The S-shaped diffuser was one of the most popular standard varieties of curved diffusers. In this diffuser, the generation of terribly capable pressure was driven by streamwise vortices because of the curvature in the flow's direction. The research on the S-shape diffuser was primarily concerned with the static pressure recovery coefficient and the turning angle effect. The investigation of the performance of a curved diffuser and the measurement of various parameters has been a priority for researchers since the beginning of the 21st century. The flow in the curved diffusers was complicated due to infiltration in the curvature in the flow direction. Kline

and Fox [1] explored the fluid flow regimes of a curved diffuser. They concluded that flow regimes are determined by the ratio of centre line radius to throat width, turning angle, and area ratio. They also concluded that there was a fast drop off in the allowable ratio of the area for the primary stall limit as the turning angle was increased. R.W. Fox et al. [2] carried out work on the S-shape diffusers and another study of variables in two-dimensional channel diffusers. The curve's geometry was an arc with a linear distribution of area that is normal to the midline. As a result, they generated a graph of flow regimes for an unstalled and stalled S-shape diffuser for flow to turn an angle of 0°- 90° with a step difference of 10°. Bansod and Bradshaw [3] studied the flow in several S-shaped diffusers. They formulate the generation of contra-rotating vortices. They showed that the region of low pressure at the exit is due to the vortices carrying free stream flow into the boundary layer. Wellborn et al. [4] represented a benchmark for aerodynamic statistics for compressive flow through a curved diffuser. According to the research, the duct's curvature allows for significant pressure-driven secondary flows that transform into counter-rotating vortices. These findings indicate that stream-wise flow separation occurs within the passage. Hingst and Wendt [5] presented the results of vortex formations shed by a low-profile vortex generator. The vortex generator's height in relation to the turbulent boundary layer varies. The counter-rotating vortex pair was seen in all of the cases. Reichert and Wendt [6] examined the impact of the vortex generator on the curved diffuser having a subsonic flow. The findings indicate that aerodynamic performance increases and flow non-uniformity at the diffuser exit decreases. Sonada et al. [7] investigated experimentally and numerically the stream qualities at intervals of S-shaped annular ducts. They have studied the effects of the two kinds of inlet boundary layers: thin and thick. The findings showed a significant change in the flow pattern at the outlet. The aerodynamic affectability of the S-formed diffuser on the channel limit layer thickness was seen to be high. Vinit Gupta et al. [8] examined the effectiveness of S-shaped diffusers by utilising CFD. They investigated diffusers with dimensions of 15°/15°, 22.5°/22.5°, 30°/30°, 45°/45°, and 90°/90° for

constant circular midline lengths of 60 cm and inlet aspect ratios of two, four, and six. When the flow's curvature increases, the flow's uniformity at the outlet decreases, and the C_{PR} decreases. As the aspect ratio of the diffuser grows, then the pressure recovery and uniformity flow decreases. Manoj K. Gopaliya et.al. [9] studied the influence of offset in the S-shape diffuser having a rectangular inlet and semicircular exhaust. The analysis shows that when the offset along the diffuser's length rises, the C_{PR} decreases. Pasha and Mujeeb [10] examined the swirl effect in a curved diffuser having an AR of 2 and an angle of turn of $22.5^\circ/22.5^\circ$. The results indicate that swirl flow at the diffuser's inlet enhanced both the pressure recovery and total pressure loss coefficients. A. Jessam et al. [11] conducted computational and experimental studies of flow control in an S-shape diffuser, including and excluding energy promoters. The simulation was done with ANSYS-FLUENT 16.2. The performed experiment had a $Re = 5.8 \times 10^4$ and a turbulence intensity of 5.0%. The use of energy boosters resulted in a drop in the separation of the outer surface boundary layer, which led to an increase in the C_{PR} and a drop in the C_{TL} .

The current study examined the effects of straight and curved diffusers, specifically $30^\circ/30^\circ$ and $45^\circ/45^\circ$ S-shaped diffusers with a 1.5 area ratio. Air is chosen as the operating fluid. To evaluate the overall performance of a straight-walled diffuser, it was compared to S-shaped diffusers. Computational and experimental studies were conducted to examine the static pressure recovery coefficient and total pressure loss coefficient at the same velocity.

II. EXPERIMENTAL SETUP

The experimental setup consists of a blower, a settling chamber, an S-shaped diffuser for measuring centerline velocity with a pitot tube, and static pressure assessed with a U-tube manometer. The stream speed/velocity modification dial on the air blower is used to control the various speeds and Reynolds numbers. The settling chamber contains a mesh screen that is used to reduce turbulence.

A 50 mm diameter PVC pipe of 4.5 m in length is coupled to the blower, and a settling chamber and three-layer mesh are attached at the entrance of the pipe to stabilise the flow. The pitot tube is fitted to the pipe just before the entrance of the diffuser in order to measure the centerline velocity using the total and static pressure. Three profiles of diffuser are created with the same area ratio of 1.5, the same centerline length but different turning angles, i.e., straight, $30^\circ/30^\circ$ and $45^\circ/45^\circ$ S-Shaped diffusers, respectively. The distance x is zero at the first hole, and 10 holes are drilled at an equal distance of 50mm with centerline measurement. Now 10 pressure taps are drilled on each side of the diffuser. There are 10, 10 pressure taps on the top, bottom, and walls respectively to assess the static pressure on them. The static pressure on the diffuser's surface was measured using 22 U-tube manometers. The pressure head difference is measured by connecting each pressure tap on the diffuser to the manometers. Each manometer has one end exposed to the atmosphere and the other end pressure-tapped, and $H_2 - H_1$ is calculated, i.e., head difference. These manometers are set at a 45° angle to the ground. An 8-layer

mesh is attached to the diffuser's end to prevent atmospheric air from entering it. The block diagram of the S-shaped diffuser experimental setup is depicted in Fig. 1, and the schematic representation of the S-shaped diffuser is presented in Fig. 2.

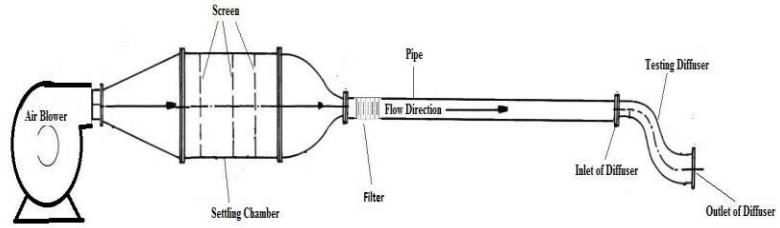


Figure 1. Experimental setup of the S-shaped diffuser.

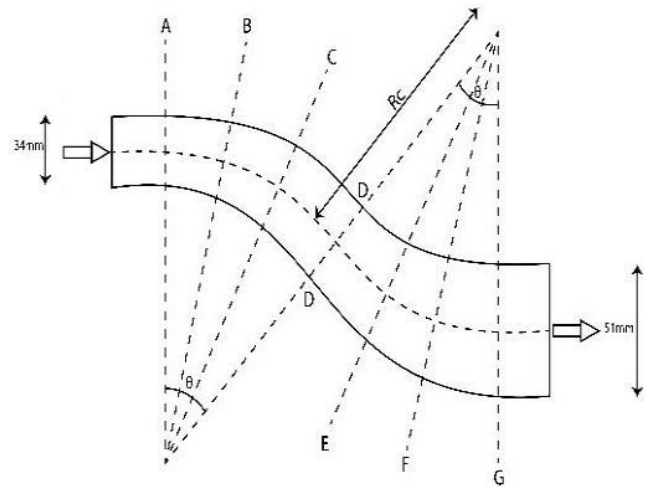


Figure 2. Schematic representation of S-shaped diffuser.

One of the fundamental techniques for maintaining instrument accuracy is instrument calibration. Calibration is the process of comparing an instrument to known standards. The mass flow rate is measured at 10 different points, and the mean values are used for further computation. As a result of changing physical parameters such as temperature, etc., the difference in mass flow rate value is $\pm 1.8\%$. A manometer reading's uncertainty is equal to ± 0.5 mm of the small scale division. The ability of the human eye to interpolate across divisions accounts for this.

III. GEOMETRICAL PARAMETERS

In the sectioned diffuser, the section was prepared with a different turn angle, i.e., $30^\circ/30^\circ$, $45^\circ/45^\circ$. Its upper and lower limbs both turn $30^\circ/30^\circ$ and $45^\circ/45^\circ$. The radius of curvature at the centerline for both upper and lower limbs is 477 mm for $30^\circ/30^\circ$, 318 mm for $45^\circ/45^\circ$, and the centerline length is 500 mm with a diffuser outlet area ratio of 1.5. The diffuser features a square inlet and a rectangular exit. The width was similarly disseminated along the 500 mm centerline length. The sectioned S-shaped diffuser was divided into six sections according to the turn angle and curvature radius. The inlet velocity is assessed using a pitot-static tube placed in front of the diffuser's inlet portion in the direction of fluid flow.

IV. GOVERNING EQUATION

The continuity equation is always based on the principle of conservation of the mass of fluid. Consider a steady-state flow field in two dimensions on an incompressible fluid.

The equation for mass conservation in coordinates.

$$\frac{\partial u}{\partial x} + \frac{\partial v}{\partial y} + \frac{\partial w}{\partial z} = 0 \quad (1)$$

X-Momentum equation:

$$u \frac{\partial u}{\partial x} + v \frac{\partial u}{\partial y} + w \frac{\partial u}{\partial z} = -\frac{1}{\rho} \frac{\partial p}{\partial x} + \nu \left[\frac{\partial^2 u}{\partial x^2} + \frac{\partial^2 u}{\partial y^2} + \frac{\partial^2 u}{\partial z^2} \right] + \frac{1}{\rho} \left[\left(\frac{\partial(-\rho \overline{u'u'})}{\partial x} \right) + \left(\frac{\partial(-\rho \overline{u'v'})}{\partial y} \right) + \left(\frac{\partial(-\rho \overline{u'w'})}{\partial z} \right) \right] \quad (2)$$

Y- Momentum equation:

$$u \frac{\partial v}{\partial x} + v \frac{\partial v}{\partial y} + w \frac{\partial v}{\partial z} = -\frac{1}{\rho} \frac{\partial p}{\partial y} + \nu \left[\frac{\partial^2 v}{\partial x^2} + \frac{\partial^2 v}{\partial y^2} + \frac{\partial^2 v}{\partial z^2} \right] + \frac{1}{\rho} \left[\left(\frac{\partial(-\rho \overline{u'v'})}{\partial x} \right) + \left(\frac{\partial(-\rho \overline{v'v'})}{\partial y} \right) + \left(\frac{\partial(-\rho \overline{v'w'})}{\partial z} \right) \right] \quad (3)$$

Z-Momentum equation:

$$u \frac{\partial w}{\partial x} + v \frac{\partial w}{\partial y} + w \frac{\partial w}{\partial z} = -\frac{1}{\rho} \frac{\partial p}{\partial z} + \nu \left[\frac{\partial^2 w}{\partial x^2} + \frac{\partial^2 w}{\partial y^2} + \frac{\partial^2 w}{\partial z^2} \right] + \frac{1}{\rho} \left[\left(\frac{\partial(-\rho \overline{u'w'})}{\partial x} \right) + \left(\frac{\partial(-\rho \overline{v'w'})}{\partial y} \right) + \left(\frac{\partial(-\rho \overline{w'w'})}{\partial z} \right) \right] \quad (4)$$

DIFFUSER PROFILE EQUATION

The profile equations of an S-shape diffuser were generated using the MATLAB-2017a/Simulink software. A curve fitting tool was used to generate the equation. To select the data to fit in the curve fitting tool to a selected variable for X and Y input. The polynomial approach was chosen for the fourth-degree polynomial equations because it produced the best results while employing specific coefficient constraints. With 95% confidence bounds, the unknown variables p_1 , p_2 , p_3 , p_4 , and p_5 were derived. The 45/45 S-shaped diffuser with a linear model of a 4th degree polynomial (Fig. 3).

$$f(x) = p_1 x^4 + p_2 x^3 + p_3 x^2 + p_4 x + p_5 \quad (5)$$

Coefficient of variation (with 95 percent confidence bounds):

$$p_1 = .573e-07 (-.3027e-06, .4182e-06)$$

$$p_2 = 0.0004251 (-0.003163, 0.003351)$$

$$p_3 = -0.02736 (-0.1208, 0.06566)$$

$$p_4 = 0.1558 (-0.7381, 1.05)$$

$$p_5 = 33.35 (31.1, 35.61)$$

Goodness of fit:

SSE: 0.5507

R-Square: 0.9982

Adjustment R-Square: 0.995

RMSE: 0.5247

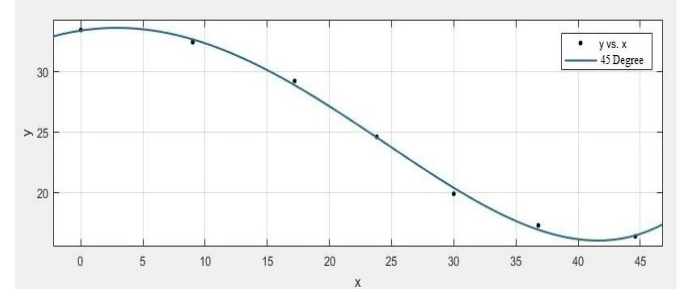


Figure 3. 45/45 S-shaped diffuser profile graph plotted by MATLABv2017.

V. COMPUTATIONAL DOMAIN AND BOUNDARY CONDITIONS

The current studies were conducted on the two-dimensional straight and S-shape diffuser computational domains. The quadrilateral cell elements have been chosen with a structure mesh scheme selected for the analysis. The meshing quality of the geometry is maintained by the skewness, wrap angle, and aspect ratio of each cell. In geometry, the aspect ratio value was less than 50, and warped cells formed an angle of greater than 45 on the cell's sides. A fine mesh is put near wall sections while keeping $y^+ < 1$. The initial mesh node is set 0.04 mm away from the surface. Boundary layer meshing was used near walls to precisely capture the viscous sub-layer, velocity gradient, and flow separation. After mesh generation, the quality of the grid was checked in the ANSYS Fluent module. Table 1 represents the boundary conditions of the fluid at the inlet of the diffuser.

Table 1. Boundary conditions at inlet

Velocity (m/s)	Re	$\rho_{\text{air}} (\text{kg/m}^3)$	$\rho_{\text{water}} (\text{kg/m}^3)$	μ in Pa
23.6	53490	1.2	1000	1.8e-5

VI. GRID INDEPENDENCY TEST

The grid independence test was used to examine the change in maximum static pressure as a function of grid size. The size of the element lies between 0.9 mm to 4 mm. The standard k- ϵ turbulence model was used with quad meshing. There is no change in static pressure for grid sizes of 0.9 mm and 1 mm. As a result, the current investigation employs a grid size of 1 mm. The maximum static pressure results produced from the study nearly closed the experimental results (Fig.4).

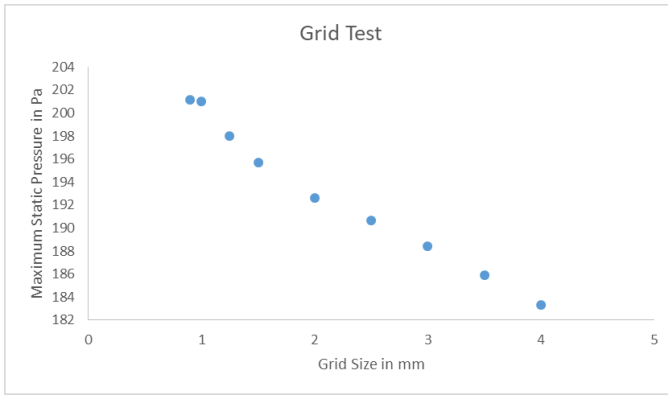


Figure 4. Comparison of static pressures with mesh sizes ranging from 0.9 mm to 4 mm.

VII. PERFORMANCE PARAMETER

The S-shape diffuser's performance was tested by means of static pressure recovery coefficient and total pressure loss coefficient.

STATIC PRESSURE RECOVERY COEFFICIENT (C_{PR})

It is characterized by the exchange of kinetic energy by extent into pressure energy because of diffusion at any cross sectional area along the diffuser's length [12].

$$C_{PR} = \frac{P_{so} - P_{si}}{\frac{1}{2} \rho u^2}$$

Where P_{so} and P_{si} represent the mass weighted average static pressures at the exit and inlet, respectively, and u represents the average inlet velocity.

TOTAL PRESSURE LOSS COEFFICIENT (C_{TL})

It is described as the amount of total pressure loss as a result of viscous forces and turbulent intermixing to the mean inlet dynamic pressure [12].

$$C_{TL} = \frac{P_{ti} - P_{to}}{\frac{1}{2} \rho u^2}$$

Where P_{ti} and P_{to} denote the total pressure at the inlet and outlet, respectively.

VIII. RESULTS AND DISCUSSION

The static pressure contours for straight wall diffuser and S-shaped diffusers with different turning angles are shown in Figs. 5-7. The fluid flows in a straight diffuser in a linear motion, and another diffusers has a different turning angle, so the fluid is guided by a curved profile. The figures illustrate that static pressure rises throughout the diffuser's length. It is noteworthy that with the change in turning angle from 0° to 45° , the flow diverts from convex wall to concave wall. The

blowing of the stream brings about a leave misdistribution with the higher flow velocity outwardly of the curvature.

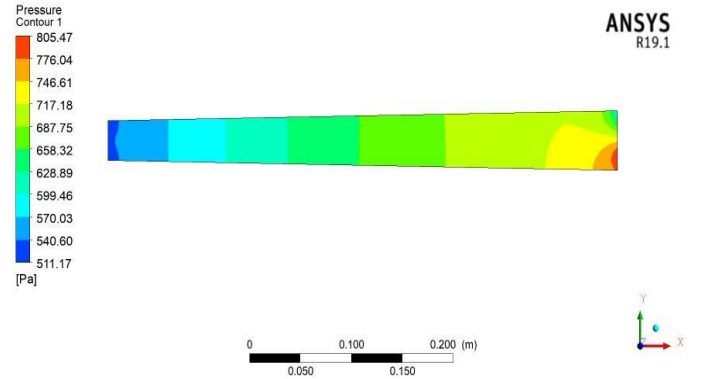


Figure 5. Static pressure contour of straight walled diffuser at 23.6 m/s.

The flow structure in an S-shaped diffuser was distinguished by two distinct zones. One was the inviscid flow, and another was a thin boundary layer through the first curve of the S-shaped diffuser. The centrifugal force proportional to $\rho U^2/2$ produces a pressure gradient. The centrifugal force generated by the flow being turned off is balanced by this pressure gradient. As a result, the outside of the curvature has more pressure than the inside, and the total pressure increases measured along the lower surface were accurately predicted by the analysis. Pressure is low at the entrance due to flow separation, but increases as it passes through the reattachment zone.

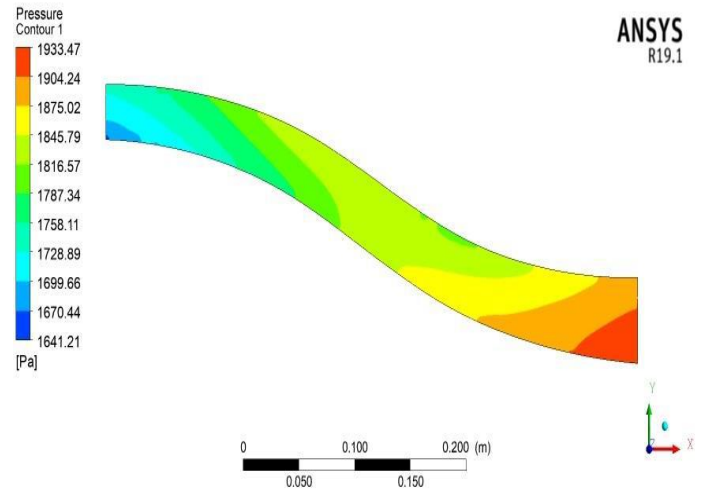


Figure 6. Static pressure contour of 45/45 S-shaped diffuser at 23.6 m/s

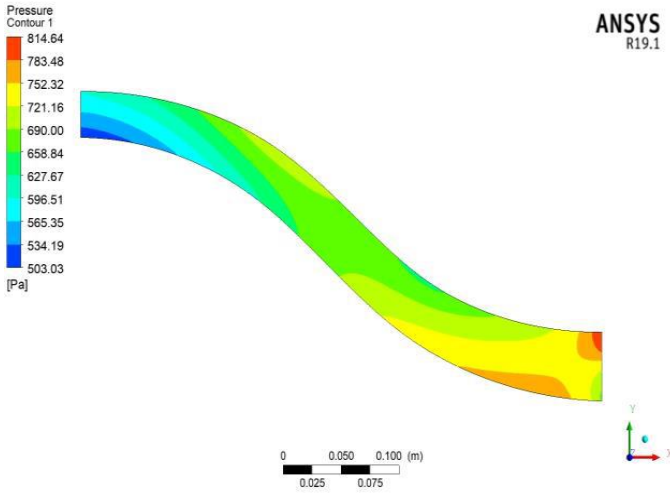


Figure 7. Static pressure contour of 45/45 S-shaped diffuser at 23.6 m/s

Lip separation was observed at the diffuser's entrance. The bends of the diffuser also caught stream-wise flow separation zones. The separation of flow was one of the major contributions to the pressure drop with the secondary flow. Due to the spatial pressure variation, the secondary flow structure was appeared. The flow distortion and loss of pressure were observed at the interfacial plane. It was discovered that lip separation enhances the effect of flow separation within the diffuser. The distribution of turbulence intensity across the total plane is more or less uniform at the exit. At the diffuser exit, this indicates a uniform flow distribution.

IX. STATIC PRESSURE RECOVERY COEFFICIENT (CPR)

The variations of the coefficient of pressure recovery throughout the diffuser length are depicted in Fig. 8. The mass averaged C_{PR} continuously improves in straight wall diffusers, whereas the pressure recovery coefficient rises in the first bend of the curved diffusers, i.e., 30°/30° and 45°/45°. The second bend has a decrease in recovery coefficient near the start of the turn in the plane because of a change in curvature direction, which causes turbulent intermixing. After the turn, the C_{PR} gradually increases to the exit of the duct.

As a result, in order to have the best understanding of the flow at the outlet, it is non-uniform. The static pressure recovery coefficient of straight-wall diffusers and S-shaped diffusers increases constantly along their length. When C_{PR} is compared to a straight-walled diffuser, then C_{PR} drops by 4.54 percent for 30°/30° and 9.38 percent for 45°/45° S-shaped diffusers as a result of flow separation increasing with turning angle. A separation zone is found near the first bend in all diffusers and continues around the second bend's outside surface.

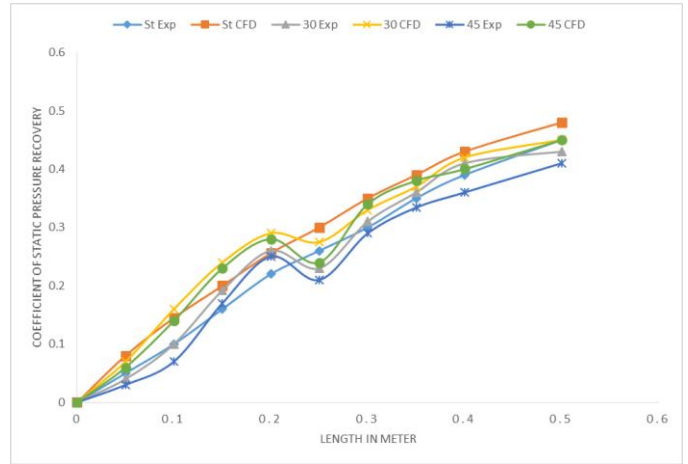


Figure 8: Comparison of static pressure recovery coefficient over the length of the diffuser at 23.6 m/s.

X. TOTAL PRESSURE LOSS COEFFICIENT (C_{TL})

The variation of the averaged mass flow rate at the coefficient of total pressure loss is depicted in Fig. 9. All diffusers have a continuous rise in total pressure loss coefficient, but the 30°/30° and 45°/45° S-shaped diffusers have a sudden increase in static pressure loss coefficient at the end of the first curve and the beginning of the second curve. The fluids gain back their lost energy, and the coefficient of loss is practically constant until they reach the diffuser outlet. When the bend begins, it introduces centrifugal force into the fluid flow. The 45°/45° S-Shaped diffuser exhibits the highest C_{TL} .

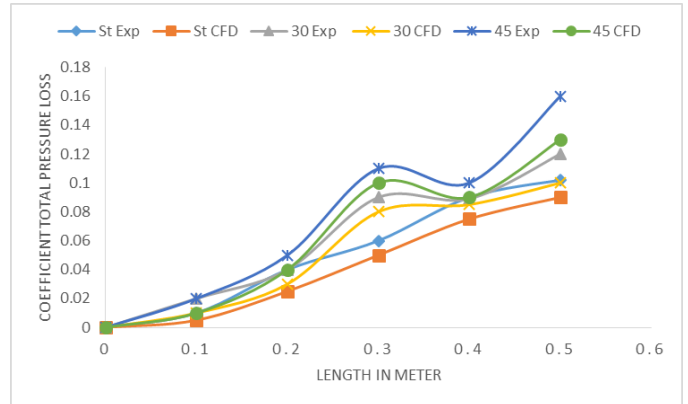


Figure 9: Comparison of the total loss pressure coefficient over the length of the diffuser at 23.6 m/s.

Fig. 9 illustrates that average C_{TL} improves by 16.21 percent for a 30°/30° S-shaped diffuser and by 44.27 percent for a 45°/45° S-shaped diffuser in comparison to a straight-wall diffuser. The high centre velocity was accelerated to the diffuser surface's concave region, as a result of turbulence, energy is exchanged between streamlines. The high-velocity flow was directed to a concave area of the diffuser surface, as a result of which a complex flow pattern is formed.

XI. COMPARISON OF EXPERIMENTAL AND COMPUTATIONAL RESULTS

Experimental work has been conducted to verify the computational results for two different diffuser profiles. Inlet velocity was determined experimentally and used as an input to the computational analysis. Table 2 illustrates the validation of experimental and computational results for the static pressure recovery coefficient at the diffusers' outlet condition. The standard k-ε model is used to predict C_{PR} in the diffuser that is closer to the experimental C_{PR} . The loss coefficient computational results are also close to the experimental results, as shown in Fig. 9.

Table 2. Comparisons of experimental and computational results of the diffusers

Velocity (m/s)	Straight Exp. C_{PR}	Straight CFD C_{PR}	Error %	45/45 S-Shaped Exp.	45/45 S-Shaped CFD	Error %
23.6	0.42	0.43	2.3	0.37	0.41	10.8

CONCLUSION

The following conclusions can be drawn based on the current investigation:

- Both experimental and computational results show that fluid shifted towards the outer wall because of the generation of secondary motion that was caused by the combined effects of centrifugal action of the centerline curvature and an adverse pressure gradient.
- The pressure recovery coefficient for 30°/30° and 45°/45° diffusers drops with an increase in turning angle.
- It was seen that there was a loss of performance in the S-shaped diffuser because of the flow separation and secondary flow.
- The change in curvature caused a decrease in the rate of static pressure recovery coefficient at the inflection plane.
- There is an exit misdistribution in the flow with a high stream velocity on the outside of the flow turning due to the bend in the diffuser.
- The findings show that maximum performance is observed in the straight wall diffuser in comparison to the 30°/30° and 45°/45° diffusers.
- The fluid was propelled at high speed to the concave section of the S-shaped diffuser.

Abbreviations

P	Pressure
V	Velocity
C_{PR}	Static pressure Recovery coefficient
C_{TL}	Total pressure loss coefficient
ρ	Fluid density
R_e	Reynolds Number
AR	Area Ratio

AS	Aspect ratio
W_o	Width of Outlet
D_h	Hydraulic Diameter at the inlet
μ	Viscosity of working fluid
RMSE	Root mean squared error
SSE	Sum of Squares due of error

REFERENCES

- [1] Kline, S. J., Abbott, D.E., and Fox, R.W., "Optimum Design of straight walled diffusers", *Journal of Basic Engineering*, pp 321-331, Sept. 1959
- [2] Fox, R.W., & Kline, S.J., "Flow Regimes in Curved subsonic diffusers", *Journal of Fluid Engineering*, Vol 84(3), pp 303-312, 1962
- [3] Bansod, P., and Bradshaw, "The Flow in S-Shaped ducts" *Aeronautical Quarterly*, Vol 23 pp 140-141, 1970
- [4] Wellborn, S.R., Reichert, B.A., and Okiishi, "An Experimental Investigation of the flow in diffusing S-duct," *AIAA paper 92-3622*, 1992
- [5] Hingst, W.R., and Wendt 1994, "Flow Structure in the Wake of Fishbone vortex generator", *AIAA Journal*, Vol 32, No 11, PP 2234-2240, 1994
- [6] Reichert, B.A., and Wendt, B.J., 1996, "Improving Curved Subsonic Diffuser with Vortex Generators", *AIAA Journal*, Vol-34, No -1, PP 65-72, 1996
- [7] Sonada, T., Arima, T., and Oana, "The Effect of Inlet Boundary layer Thickness on the flow within an annular S-Shaped duct," *Journal of Turbomachinery*, Vol-121, PP 626-634, 1999
- [8] Vinit Gupta, Rajneesh Devpura, S.N. Singh & V Seshadri, "Effect of aspect ratio and curvature on Characteristics of S-Shaped diffusers", *Indian Journal of Engineering & Material Sciences*, Vol. 8, pp. 141-148, June 2001
- [9] M.K. Gopaliya, M. Kumar, S. Kumar, S.M. Gopaliya, "Analysis of performance characteristics of the S-shaped diffuser with offset," *Aerospace Science and Technology* 11, 130-135, 2007
- [10] Pasha, R. J., & Mujeeb, A. (2013). CFD simulation of swirling effect in s-shaped diffusing duct by swirl angle of 10. *Journal of Mechanical and Civil Engineering*, 6(2), 11-19.
- [11] Raed A. Jessam, Hussain H. Al-Kayiem, Mohammed S. Nasif, "Flow control in S-Shaped air intake diffuser of the gas turbine using proposed energy promoters", *MATEC Web of Conferences*, Vol. 131, Sept 2017
- [12] M.K. Gopaliya, P. Jain, S.K., V. Yadav, S. Singh (2014). Performance Improvement of an S-Shaped diffuser using moment imparting technique, *ISOR Journal of Mechanical and Civil* 11(3),23-31.